Fernández Villanueva, E.; Boronat Zaragoza, M.; Corma Canós, A. (2020). The Crucial Role of Cluster Morphology on the Epoxidation of Propene Catalyzed by Cu-5: A DFT Study. The Journal of Physical Chemistry C. 124(39):21549-21558. https://doi.org/10.1021/acs.jpcc.0c06295

# The crucial role of cluster morphology on the epoxidation of propene catalyzed by $Cu_5$: a DFT study

Estefanía Fernández, Mercedes Boronat,* and Avelino Corma

Instituto de Tecnología Química, Universitat Politècnica de València - Consejo Superior de Investigaciones Cientificas, Av. de los Naranjos, s/n, 46022 Valencia, Spain

*Supporting Information*

**ABSTRACT:** The selective oxidation of propene to propene oxide (PO) is an industrially relevant and still challenging reaction that requires the design of highly specific catalysts able to improve simultaneously activity and selectivity. Metallic copper exhibits high selectivity towards propene epoxidation that drops when the catalyst surface is oxidized under reaction conditions. Based on previous work showing that small planar $Cu_5$ clusters are more resistant to oxidation than 3D ones, we have performed a detailed theoretical study of the mechanism of propene oxidation with molecular $O_2$ and atomic O adsorbed on both planar and 3D $Cu_5$ clusters. The desired pathways leading to PO as well as the undesired routes producing propanal, acetone, or allyl intermediates that finally evolve to acrolein or $CO_2$ have been considered, and the global analysis of all data indicates that planar $Cu_5$ clusters are promising candidates for the selective epoxidation of propene.

**KEYWORDS:** DFT, propene, epoxidation, mechanism, clusters, structure-activity relationship

## 1. INTRODUCTION

Propene or propylene oxide (PO) is an important industrial precursor of polyurethane and other unsaturated polyesters, and it is used in the manufacture of commercial products such as foams, adhesives, food additives or cosmetics, among others. The current industrial processes to synthesize PO are broadly divided into those employing chlorohydrin compounds, which generate stoichiometric amounts of chloride salts, and those using organic hydroperoxides that result in co-production of too large amounts of tert-butyl alcohol or styrene monomers, with the associated marketing and production problems.[1–4] A greener route generating water as the only by-product is the direct epoxidation of propene with hydrogen peroxide using titanium silicalite (TS-1) as catalyst, but its commercial use is hindered by the cost and dangers associated to high concentrations of $H_2O_2$.[4,5] To overcome these limitations, the in situ synthesis of $H_2O_2$ from $H_2$ and $O_2$ has been attempted, and good selectivity to PO has been reported using catalytic systems composed by Ag, Au, or bimetallic Au-Cu, Au-Pd and Pd-Pt nanoparticles supported on Ti-containing materials, although at propene conversion below 10%.[6–11] Alternatively, the direct epoxidation of propene using molecular $O_2$ as the only oxidant has received increasing attention because of the successful application of this reaction to the industrial production of ethene epoxide over promoted silver catalysts.[12–14] However, the use of silver for propene epoxidation is not efficient, and despite extensive investigation on the influence of particle size, morphology or crystallographic plane exposed, propene conversion or selectivity to PO are usually low.[1,2,15–19]

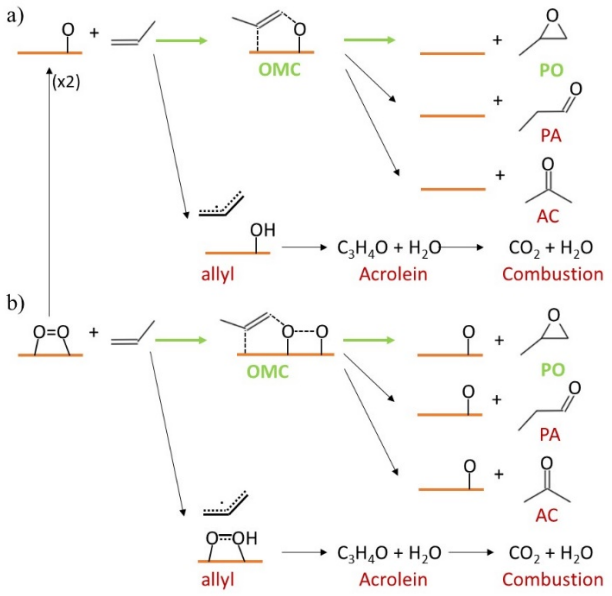


**Scheme 1.** Propene epoxidation mechanism by adsorbed a) atomic oxygen or b) molecular oxygen.

This is so because the mechanism of propene oxidation on metal surfaces (Scheme 1a) requires the initial dissociation of molecular $O_2$ into atomic O. Then, by reaction of propene with an adsorbed O atom, an oxametallacycle (OMC) intermediate precursor is first

obtained, which then reorganizes to produce PO. However, the adsorbed O atom can also capture one hydrogen atom from the methyl group of propene, producing a highly reactive allyl species that is converted into acrolein and, depending on the reaction conditions, to $CO_2$. Moreover, even if the OMC is successfully reached, its rearrangement can also lead to propanal (PA) or propanone (acetone, AC), thus lowering the final selectivity to PO. The initial selectivity to OMC or allyl intermediates is determined by the electrophilic/nucleophilic character of the surface oxygen atoms, which depend on the metal employed and on the degree of oxidation of the metal surface. Thus, it was theoretically proposed that Cu(111) is intrinsically more selective than Ag(111) and Au(111) because it favours the formation of the OMC intermediate against hydrogen abstraction,[20,21] and it was indeed experimentally confirmed that metallic copper exhibits a high selectivity towards epoxidation, but it drops when the catalyst surface becomes oxidized.[22–24] Marimuthu et al. found that the light-induced reduction of the surface Cu atoms of a partly oxidized $Cu/SiO_2$ catalyst increased the selectivity to propene epoxide from 20 to 50% under propene oxidation operating conditions.[24] Going one step further, a number of experimental[25–27] and theoretical[28–30] studies have demonstrated that metallic $Cu^0$ and some $Cu^+$ species in small clusters or in $Cu_2O(110)$ facets are selective to PO, while the $Cu_2O(111)$ planes present in large particles preferentially catalyse the formation of acrolein. It is clear that a strict control of the copper oxidation state is necessary in order to selectively catalyse the epoxidation of propene. We have recently shown that it is possible to stabilize metallic $Cu^0$ species by adjusting the atomicity of small $Cu_n$ clusters.[31–33] More specifically, the electronic structure of clusters with five atoms or less ($\leq Cu_5$) renders them planar and more resistant to oxidation because of the high energy barrier involved in the dissociation of molecular $O_2$. In this case, the direct reaction of propene with molecular $O_2$ (Scheme 1b) might change the relative rates of OMC and allyl intermediate formation, leading to a different selectivity. In this work we study computationally the mechanism of propene epoxidation and competing reactions on $Cu_5$ clusters with planar and 3D geometries. The key role of cluster morphology on the electronic structure and therefore on the catalytic behavior of small copper clusters is demonstrated, and planar $Cu_5$ species are proposed as good candidates for the selective oxidation of propene to PO with molecular $O_2$.

## 2. COMPUTATIONAL DETAILS

All calculations in this work are based on density functional theory (DFT) and were carried out with the Gaussian 09 program package.[34] The B3PW91 functional was employed, which combines the PW91 correlation functional by Perdew and Wang with Becke's hybrid three-parameter exchange functional.[35] The Def2TZVP[36,37] basis set was used for Cu atoms because of its good performance at an affordable computational cost, whereas the standard 6-311+G(d,p) basis set by Pople was employed for O, C and H atoms.[38] In all cases, the positions of all atoms in the system were fully optimized without any restriction, and all stationary points were characterized by pertinent frequency analysis calculations. Transition states were determined through potential energy surface (PES) scans along with the subsequent optimizations and vibrational frequency calculations. Atomic charges and molecular orbital distributions were calculated using the natural bond order (NBO) approach.[39].The MOLDEN,[40] Jmol[41] and ChemCraft[42] programs were used throughout the work to visualize the systems and their frequencies, and to obtain a graphical representation of their molecular orbitals.

## 3. RESULTS AND DISCUSSION

### 3.1. Adsorption of propene and $O_2$ on planar and 3D $Cu_5$ clusters

The adsorption of one molecule of propene on the two lowest energy isomers of $Cu_5$ (planar and 3D) generates structures **1** and **2** in Figure 1a. Propene adsorbs weakly on the two-atoms edge of planar $Cu_5$ and more strongly on top of one corner Cu atom on 3D $Cu_5$ (Figure 1a), and in both cases the coordination of the alkene to the metal cluster is preferentially established through one copper atom only. The interaction of propene with the cluster involves a transfer of electron density from the $\pi$ orbital of the molecule to empty *3d* orbitals of the cluster, and some back-bonding from a different *3d* orbital of the copper cluster to the $\pi^*$ anti- bonding orbital of the molecule. As a result, the double bond of propene gets elongated by 0.043 and 0.047 Å in **1** and **2**, respectively, and the cluster gets a little bit oxidized, with a net charge transfer of 0.07e in **1** and 0.03e in **2**. The slightly larger elongation of the C=C bond in structure **2** correlates with the larger adsorption energy, and the lower net charge implies a larger contribution from back-bonding, in agreement with the lower HOMO-LUMO energy gap of 3D $Cu_5$ (Figure 1b).

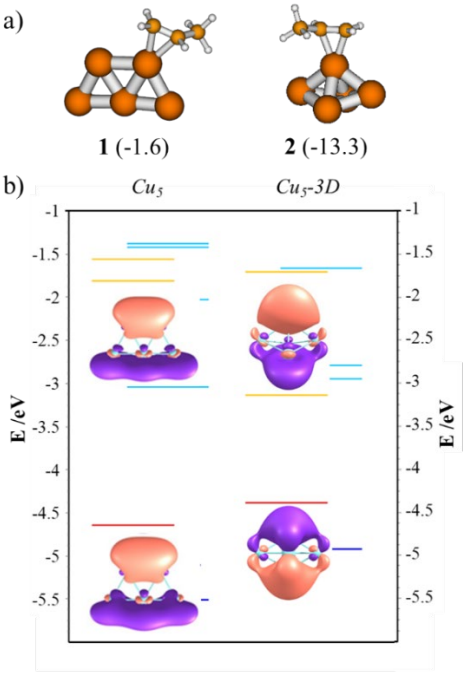


**Figure 1.** a) Optimized structures and adsorption free energies in parenthesis (in kcal $mol^{-1}$) of propene adsorbed on planar and 3D $Cu_5$ clusters. Cu, C and H atoms are depicted in orange, amber, and white, respectively. b) Stability and composition of the highest occupied and lowest unoccupied molecular orbitals (HOMOs and LUMOs) of the two $Cu_5$ isomers calculated at the B3PW91/6-311+G(d,p) level (eV).

The most stable geometries for an $O_2$ molecule adsorbed on planar and 3D $Cu_5$ clusters are structures **3** (Figure 2) and **17** (Figure 3), and their corresponding adsorption free energies are -25.0 and -18.5 kcal $mol^{-1}$, as described in previous works.[31,32] Adsorption of propene is clearly weaker than that of $O_2$, and therefore structures **3** and **17** with $O_2$ already adsorbed on the metal clusters were taken as the starting situation to study the co-adsorption of the reactants. In addition, the second most stable conformation found for $O_2$ adsorbed on 3D $Cu_5$, corresponding to a *h-111* adsorption mode (structure **24** in Figure 4, 5.2 kcal $mol^{-1}$ higher in energy than **17** in Figure 3), and the system obtained after $O_2$ dissociation into two adsorbed oxygen atoms with an activation energy of 15.8 kcal $mol^{-1}$, (structure **47** in Figure 5), were used as starting reactant systems to investigate the reaction mechanism.

Note that, as advanced in the introduction, the electronic structure of the two different $Cu_5$ isomers is what causes the different stabilization and activation of $O_2$. Since the frontier orbitals for planar $Cu_5$ spread along the edges (Figure 1b), the less activated *bridge* mode (structure **3**) is preferentially formed on this $Cu_5$ isomer, whereas the 3D $Cu_5$ cluster can stabilize more activated *h-111* modes (structure **24**), which are more basic.[31]

### 3.2. OMC vs. allyl formation on planar and 3D $Cu_5$ clusters

The adsorption of propene on a planar $Cu_5$ cluster with $O_2$ strongly adsorbed on the edge, structure **3** in Figure 2, implies a non-negligible distortion of the cluster geometry (structures **4**, **11** and **14** in Figure 2) and therefore requires about 4-5 kcal mol$^{-1}$. Once this adsorption of propene close to $O_2$ is achieved, paths divert into those leading to the undesired allyl (red arrows) and to the OMC pursued (green arrows). When propene adsorbs with the methylated carbon facing the $O_2$ molecule, as in structures **4** and **11**, the system evolves through transition state TS **5**, where the $O_2$ is tilted over the cluster's edge and about to bond with the methylated carbon atom. This process leads to the four-member cycle of structure **6** with activation energy barriers of 19.1 and 19.6 kcal mol$^{-1}$ from structures **4** and **11**, respectively. The four-member cycle in **6** is easily transformed, with an activation barrier of 0.8 kcal mol$^{-1}$, into a five-member cycle or OMC intermediate where the two oxygen atoms participate (structure **8** in Figure 2). Alternatively, abstraction of hydrogen from the methyl group of structure **4** through TS **9** needs a high activation energy of 27.1 kcal mol$^{-1}$ and, when starting from the close in energy structure **11,** the activation barriers are 26.6 or 22.2 kcal mol$^{-1}$ depending on which oxygen atom participates (TSs **9** and **12**, respectively). In all cases, very stable systems containing an allyl fragment and a hydroperoxide group strongly attached to the $Cu_5$ cluster (structures **10** and **13**) are obtained. However, if propene adsorbs on structure **3** in such a way that the non-methylated carbon faces the oxygen molecule, as in structure **14**, then the path towards the allyl is impeded because the methyl group is inevitably too far to react. The calculated activation energy for the production of the OMC intermediate **16** through TS **15** is of 16.7 kcal mol$^{-1}$ only.

Co-adsorption of propene with $O_2$ already adsorbed in a *bridge* mode on the 3D $Cu_5$ cluster (structure **17** in Figure 3) is, at difference with planar $Cu_5$, thermodynamically favoured by 5.9 and 4.8 kcal mol$^{-1}$ (structures **18** and **23** in Figure 3, respectively) depending on the relative orientation of $O_2$ and the methyl group of propene. From structure **18**, the pathway towards the allyl species through TS **21** requires a higher activation energy (27.3 kcal mol$^{-1}$) than the route for OMC formation via TS **19** (22.2 kcal mol$^{-1}$). In addition, the OMC intermediate **20** has more interacting points with the cluster, at the non-methylated carbon and at both O atoms. As consequence, the difference in stability between the OMC and allyl products formed on 3D $Cu_5$ is not as large as that obtained on planar $Cu_5$. The adsorption of propene with the non-methylated carbon facing an O atom (structure **23**) is slightly less stable and, when the formation of an OMC is explored, the 3D cluster deforms into the planar geometry of TS **15** previously found and an activation energy barrier of 13 kcal mol$^{-1}$ is obtained.

A large number of structures similar in energy can be obtained by co-adsorption of propene close to $O_2$ already adsorbed in a *h-111* mode on 3D $Cu_5$ (structure **24** in Figure 4), and we chose four representative ones to follow their reactivity, namely structures **25**, **32**, **40** and **44** in Figure 4. In the highly stable structure **25** (Figure 4a), $O_2$ and propene molecules are bridged by an almost detached Cu atom that lies at almost the same distance from the two doubly bonded carbon atoms. Despite two possible OMC intermediates can be obtained starting from **25**, the attack of O to the methylated carbon of propene is clearly preferred both kinetically (activation energies of 37.1 kcal mol$^{-1}$ through TS **26** vs 26.1 kcal mol$^{-1}$ through TS **28**) and thermodynamically (structures **27** vs **29**). On the other hand, the reaction towards the allyl intermediate **31** is highly exothermic and kinetically affordable in spite of the further detachment of the Cu atom in the corresponding TSs **30**.

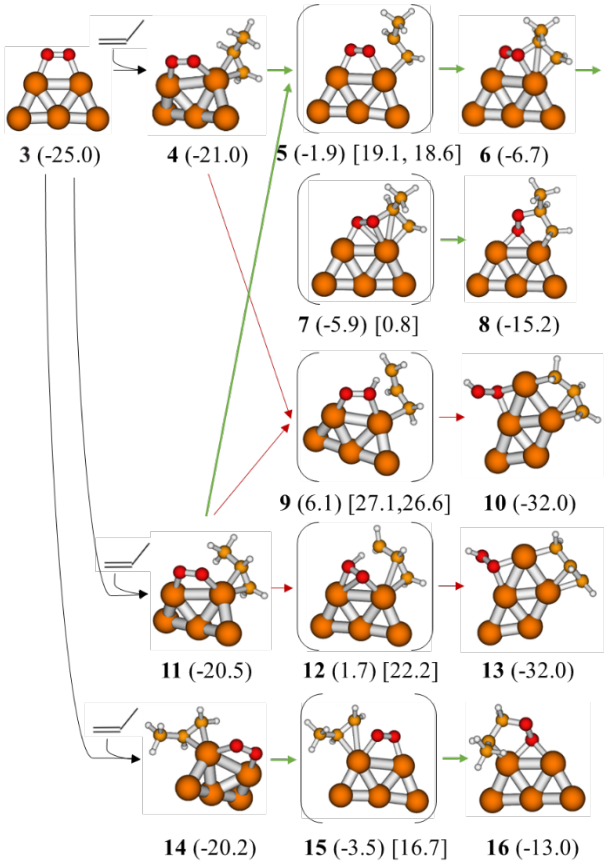


**Figure 2.** Optimized structures involved in the formation of OMC or allyl intermediates on planar $Cu_5$ clusters. Relative Gibbs free energies with respect to separate planar $Cu_5$+$O_2$+2$C_3H_6$ (in parenthesis) and activation Gibbs free energies for elementary steps (in square brackets) in kcal mol$^{-1}$. Cu, C, O and H atoms depicted in orange, amber, red and white, respectively.

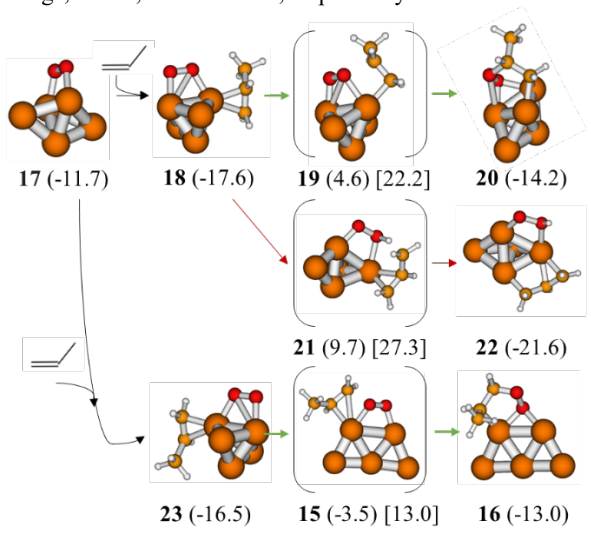


**Figure 3.** Optimized structures involved in the formation of OMC or allyl on 3D $Cu_5$ clusters. Relative Gibbs free energies with respect to separate planar $Cu_5$+$O_2$+2$C_3H_6$ (in parenthesis) and activation Gibbs free energies for elementary steps (in square brackets) in kcal mol$^{-1}$. Cu, C, O and H atoms depicted in orange, amber, red and white, respectively.

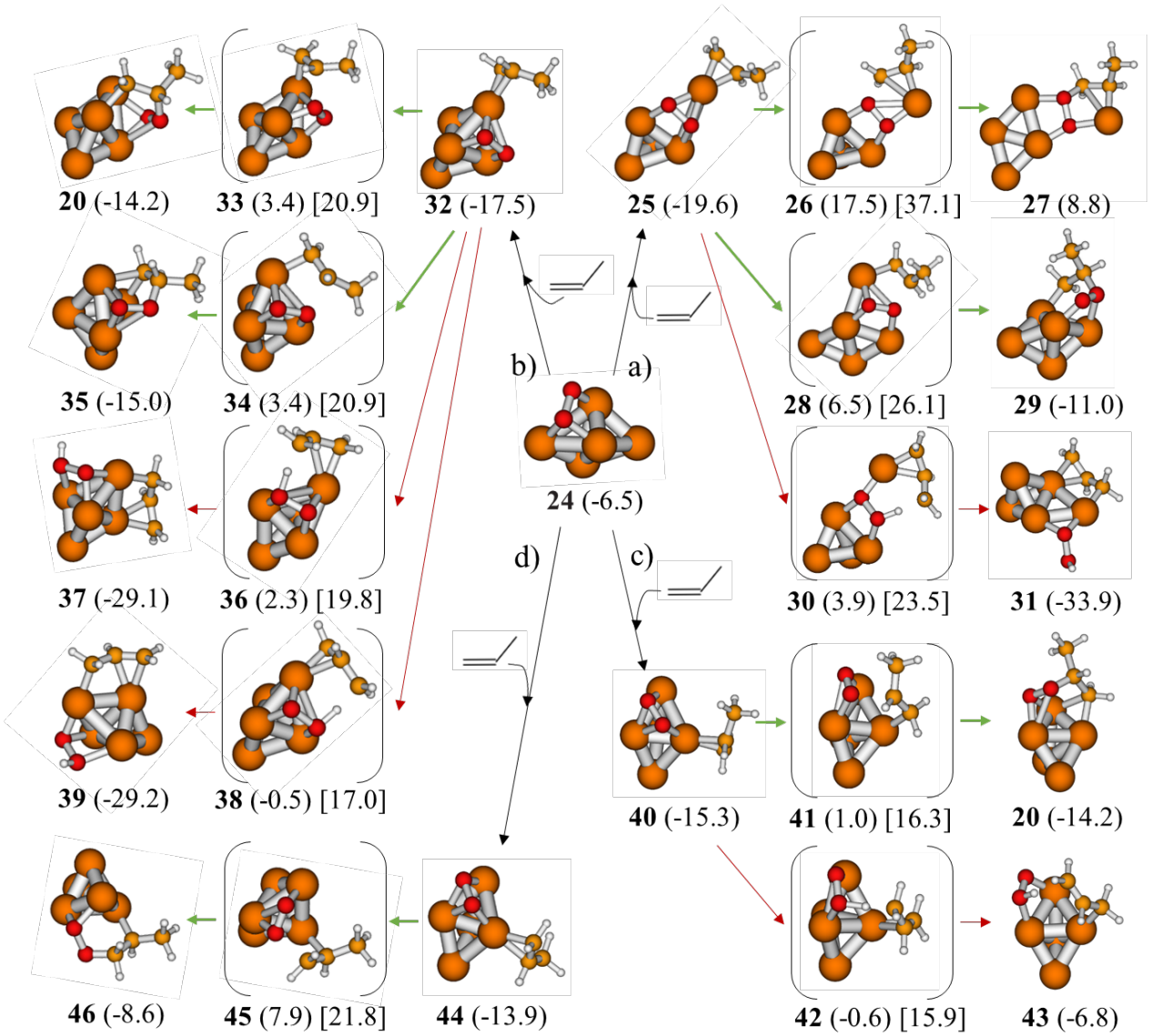


**Figure 4.** Optimized structures involved in the formation of OMC or allyl intermediates by reaction of propene with $O_2$ on adsorbed in a *h-111* mode on 3D $Cu_5$ clusters. Relative Gibbs free energies with respect to separate planar $Cu_5+O_2+2C_3H_6$ (in parenthesis) and activation Gibbs free energies for elementary steps (in square brackets) in kcal $mol^{-1}$. Cu, C, O and H atoms depicted in orange, amber, red and white, respectively.

From structure **32** (Figure 4b), there are two pathways leading to OMC formation (structures **20** and **35**) and two other ones leading to undesired hydrogen abstraction producing allyl (structures **37** and **39**). The differences between the activation energies obtained for the four steps are smaller than 4 kcal $mol^{-1}$, but the allyl species are thermodynamically more stable than the OMCs. The opposite thermodynamic trend is obtained when starting from the slightly less stable reactant structure **40** (Figure 4c). The activation energies for OMC and allyl formation are similar, 16.3 and 14.7 kcal $mol^{-1}$, respectively, but the desired OMC intermediate **20** is 7.4 kcal $mol^{-1}$ more stable than the allyl species **43**. Finally, when propene adsorbs in such a way that the methyl group is not reachable by $O_2$ (structure **44** in Figure 4d), formation of an OMC intermediate with an affordable barrier of 21.8 kcal $mol^{-1}$ is the only possible reaction step. Altogether, when $O_2$ is adsorbed in an *h-111* mode on $Cu_5$, its larger degree of activation, consistent with a superoxo species,[31,32] confers on it a more basic character that is enough to produce a slight preference towards the allyl in the propene oxidation reaction. Consistent with this, a correlation can be found between the calculated NBO charges of the reacting oxygen atom in each cluster and the selectivity to allyl formation (see Tables S1-S2 and Figure S1 of the Supporting Information).

If $O_2$ dissociates prior to the adsorption of propene, which may occur on 3D $Cu_5$,[31,32] the alkene may either adsorb close to an O atom and react following a Langmuir-Hinshelwood (LH) mechanism, or may also react directly from the gas phase with an adsorbed O atom via an Eley-Rideal (ER) mechanism (see Figure 5). In this last case, two different ER transition states were obtained that correspond to the attack of O to the methylated (TS **48**) and non-methylated (TS **51**) carbon atoms of the propene C=C double bond. The calculated activation energies are 24.5 and 23.2 kcal $mol^{-1}$, respectively, and the reaction product is in both cases the epoxide adsorbed on the cluster (structures **49** and **52**).

If the molecule is adsorbed on the cluster instead, according to a LH mechanism, either structure **54** or structures similar to **61** are obtained. Reaction starting from **61** might be possible but, since the O atom is within the structure of the cluster binding the almost separated Cu atom, barriers are likely to be high in energy and were

not studied. Starting from structure **54**, the adsorbed propene can be tilted towards one oxygen or the other to react. In TS **55** the non-methylated carbon reacts with O to produce the OMC structure **56** with an activation energy of 28.2 kcal mol$^{-1}$, whereas in TS **57** the OMC **58** is produced by reaction of O with the methylated carbon with a lower barrier of 21.0 kcal mol$^{-1}$. However, the TS **59** leading to allyl lies 9.8 kcal mol$^{-1}$ even lower in energy, requiring an activation energy of only 11.2 kcal mol$^{-1}$ for hydrogen abstraction.

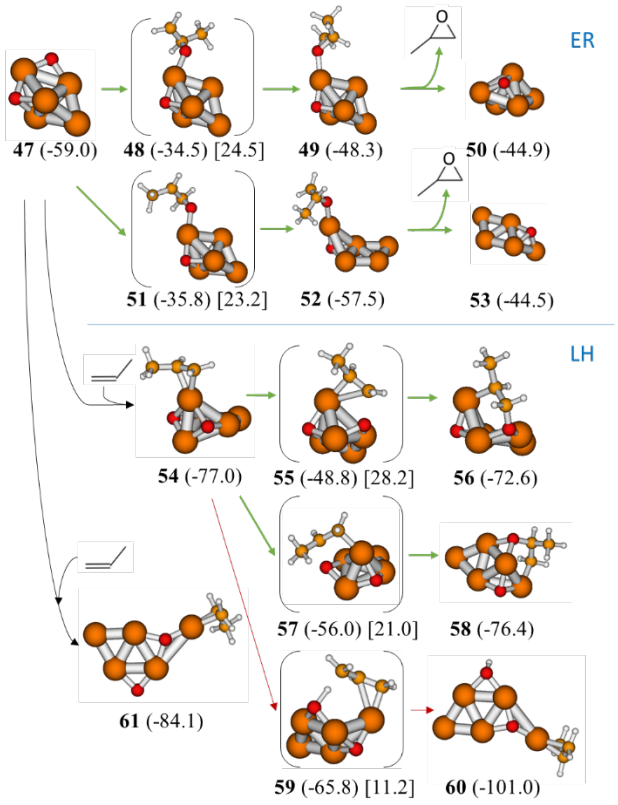


**Figure 5.** Optimized structures involved in the formation of OMC or allyl intermediates on 3D $Cu_5$ clusters with adsorbed O atoms. Relative Gibbs free energies with respect to separate planar $Cu_5$+$O_2$+2$C_3H_6$ (in parenthesis) and activation Gibbs free energies for elementary steps (in square brackets) in kcal mol$^{-1}$. Cu, C, O and H atoms depicted in orange, amber, red and white, respectively.

The lowest energy paths leading to OMC and allyl intermediates on each of the $Cu_5$ + $O_2$ systems just described are plotted together in Figure 6. It is clearly observed that formation of the desired OMC intermediate is kinetically favoured when the oxidant species is molecular $O_2$ adsorbed in a *bridge* mode, either on planar $Cu_5$ (purple lines) or on 3D $Cu_5$ (orange lines). In contrast, when $O_2$ adsorbs in a more activating *h-111* mode (green lines), allyl formation is enhanced, and this is even more so after $O_2$ dissociation (blue lines). It is also important to remark that the activation barrier for $O_2$ dissociation is larger than the energy required for production of OMC in 3D $Cu_5$ with $O_2$ adsorbed in a *bridge* mode, but smaller if $O_2$ adsorbs in a *h-111* mode, even when the $[O\cdots O]^{\neq}$ TS is higher in energy.

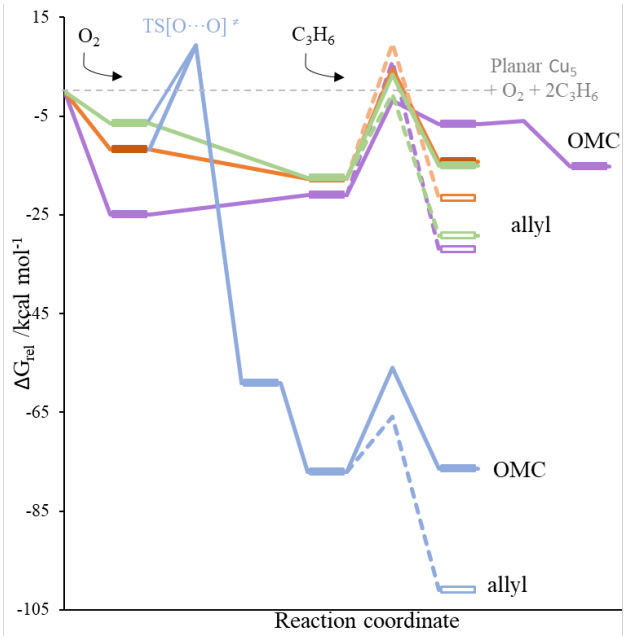


**Figure 6.** Free energy profiles for propene oxidation on planar $Cu_5$ (purple), 3D $Cu_5$ with $O_2$ adsorbed in a *bridge* mode (orange), 3D $Cu_5$ with $O_2$ adsorbed in a *h111* mode (green) and on 3D $Cu_5$ starting with $O_2$ dissociation (blue). Dashed lines indicate allyl paths. The origin of energies corresponds to separate planar $Cu_5$ + $O_2$ + propene.

All in all, the present results show that planar $Cu_5$ clusters favour the production of OMC intermediates by reaction with molecular $O_2$ due to the preferential adsorption of the latter in a not too activating *bridge* mode. However, 3D $Cu_5$ clusters are likely to perform worse in the epoxidation of propene because they are able to adsorb $O_2$ in a more activating *h-111* mode, which not only favours hydrogen abstraction but also facilitates $O_2$ dissociation. Since the preferential $O_2$ adsorption mode is determined by the different electronic structure of the two $Cu_5$ isomers, the electronic structure (and conversely, the morphology) is the ultimate feature that causes planar $Cu_5$ clusters to favour OMC production over allyl formation. The adsorbed O atoms are too basic and the pathway to allyl is greatly enhanced (see also Tables S1-S2 and Figure S1).

### 3.3. PO formation vs. competing reactions from OMC on planar $Cu_5$

Once established that planar $Cu_5$ clusters favour OMC production over allyl formation, the subsequent steps towards the target PO and the competitive reactions leading to propanal (PA) or acetone (AC) were investigated. The optimized structures involved are shown in Figures 7 and 8, and the free energy profiles for the most relevant processes are summarized in Figure 9.

From the OMC cycle of structure **8,** the direct breaking of the O-O bond and simultaneous formation of PO is not produced. Instead, two mechanisms towards PO are found (see Figure 7). In the first one (Figure 7a), the O-O bond is dissociated first through TS **62** with an activation energy of 22.4 kcal mol$^{-1}$, followed by a less energy demanding reorganization step to produce a four-centred cycle (structure **65**) that is easily converted into PO via TS **66**. In the second one (Figure 7b), the Cu-C interaction is lost after surpassing a lower barrier of 13.1 kcal mol$^{-1}$, so that an intermediate is produced where the molecule is bonded to the cluster through the $O_2$ only (structure **69**). This system reacts via TS **70** breaking the O-O bond and creating PO (structure **71**) at the same time, with a low activation energy of 9.0 kcal mol$^{-1}$.

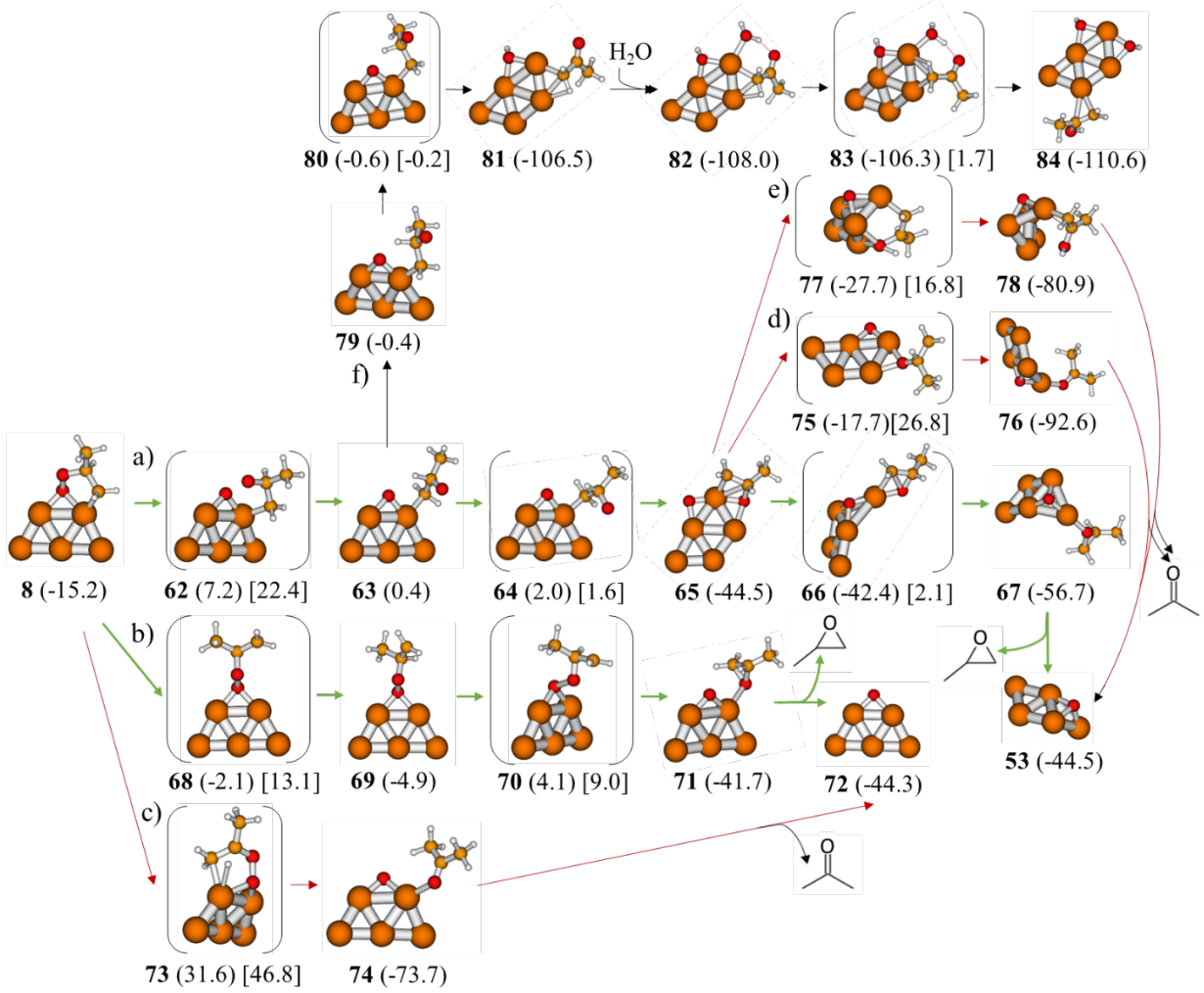


**Figure 7**. Optimized structures involved in the transformations of the OMC intermediate **8**. Relative Gibbs free energies with respect to separate planar $Cu_5+O_2+2C_3H_6$ (in parenthesis) and activation Gibbs free energies for elementary steps (in square brackets) in kcal mol$^{-1}$. Cu, C, O and H atoms depicted in orange, amber, red and white, respectively.

From structures where the O-O bond is still not dissociated, the competitive reaction leading to acetone seems unlikely because it requires the transference of the central hydrogen atom and the dissociation of the O-O bond at the same time. Indeed, trying such step from structure **8** (Figure 7c) leads to a 46.8 kcal mol$^{-1}$ activation energy (TS **73**) to produce AC (structure **74**). As a consequence, the more predominant direct path through transition state **68** is expected to enhance the selectivity towards PO.

In the search for alternative routes to obtain AC we considered structure **65** as starting point and found two possible pathways (Figure 7d, e). Direct formation of AC via TS **75** implies a barrier of 26.8 kcal mol$^{-1}$, whereas in the way through TS **77** the cluster deforms and produces the corresponding enol (2-propenol or isopropenol, structure **78**) with a smaller barrier of 16.8 kcal mol$^{-1}$. In any case, the barrier towards PO from structure **65** is only 2.1 kcal mol$^{-1}$, which indicates that formation of acetone is not competitive.

In spite of this, we noticed that the hydrogen atom next to CO in structure **63** can be favourably oriented towards the remaining O atom due to the partial positive and negative charges that they respectively present (structure **79** in Figure 7f). From here, the transfer of the hydrogen atom to the oxygen atom is extremely easy (barrierless in fact, as a -0.2 kcal mol$^{-1}$ free energy barrier is obtained, 0.7 in electronic energy) and the product is much more stable than any of the others shown because a stable hydroxyl and enolate species are formed (structure **81**). The latter could be removed as 2-propenol if it retrieves a hydrogen atom for instance through an easy reaction with water (**82-[83]-84** step).

From the OMC intermediate with the non-methylated C atoms bonded to oxygen (structure **16** in Figure 2), similar results are obtained (see Figures 8 and 9). Thus, we find a path starting with the dissociation of the O-O bond through TS **85** with an activation energy for the rate determining step of 20.2 kcal mol$^{-1}$ (Figure 8a), and a more direct pathway (Figure 8b) that starts with rupture of the Cu-C interaction via transition state **93** with an activation energy of only 6.0 kcal mol$^{-1}$. Again, competitive reactions from structures where the O-O bond is still not dissociated are equally unlikely. For instance, the reaction towards 1-propenol (structure **99** in Figure 8c) requires surpassing a barrier of 32.4 kcal mol$^{-1}$, whereas all attempts to form propanal (PA) always led to the dissociation of the O-O bond first. In addition, competitive reaction towards PA starting from intermediate species **86** (Figure 8d), **88** (Figure 8e) and **90** (Figure 8f) were always found less favourable than the alternative steps leading to PO by 4.8, 14.9 and 7.3 kcal mol$^{-1}$, respectively. To sum up, it is found that once OMC is formed on planar $Cu_5$ the subsequent steps of the mechanism towards PO production are energetically affordable, and competitive reactions generating PA or AC are always kinetically more difficult.

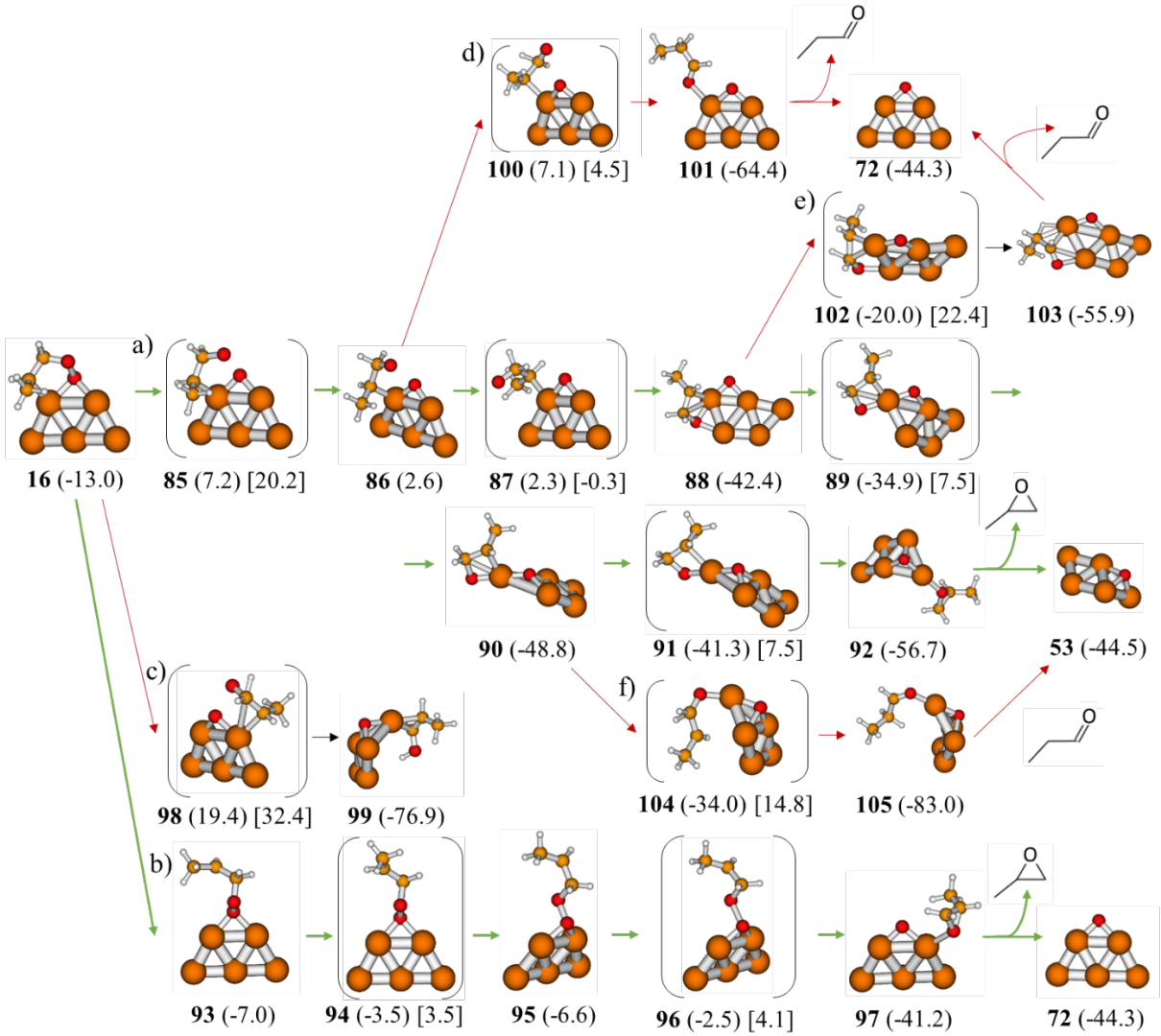


**Figure 8**. Optimized structures involved in the transformations of the OMC intermediate **16**. Relative Gibbs free energies with respect to separate planar $Cu_5$+$O_2$+2$C_3H_6$ (in parenthesis) and activation Gibbs free energies for elementary steps (in square brackets) in kcal $mol^{-1}$. Cu, C, O and H atoms depicted in orange, amber, red and white, respectively.

### 3.4. Closing the cycle: OMC vs. allyl formation on $Cu_5O$

After the formation of the first PO molecule by reaction of propene with molecular $O_2$ on planar $Cu_5$ clusters, an oxygen atom remains adsorbed on the cluster, forming a $Cu_5O$ system whose reactivity towards propene should be established in order to close the catalytic cycle. For this purpose, we studied the interaction of propene with the two $Cu_5O$ structures obtained in the first part of the cycle on planar $Cu_5$, namely, structures **72** and **53**, and the pathways leading to PO and allyl intermediates (see Figure 10).

Remarkably, reaction of propene from the gas phase following a ER mechanism with either **72** or **53** results in the direct formation of adsorbed PO (structure **107**) through the same transition state (structure **106**), with similar activation barriers of 22 kcal $mol^{-1}$.

After PO desorption, the planar $Cu_5$ cluster is retrieved to start a new and selective catalytic cycle. Co-adsorption of propene on structure **72** to start LH mechanisms is weak, with adsorption energies of only 1-3 kcal $mol^{-1}$ to form structures **108** and **111**. The activation energies to form the OMC intermediates **110** and **113** are low, 17.0 and 11.1 kcal $mol^{-1}$, respectively, and the most difficult step in the process becomes the ring closing to form the epoxide, with activation barriers of 29.0 and 36.1 kcal $mol^{-1}$ through TSs **106** and **114**, respectively. Since these barriers are rather high, the ER path leading to PO should be predominant from structure **72**. On the other hand, the possibility to form the undesired allyl intermediate by hydrogen abstraction in structure **111** requires 2.0 kcal $mol^{-1}$ more energy than OMC formation, and therefore its contribution to the total reactivity of propene should be low.

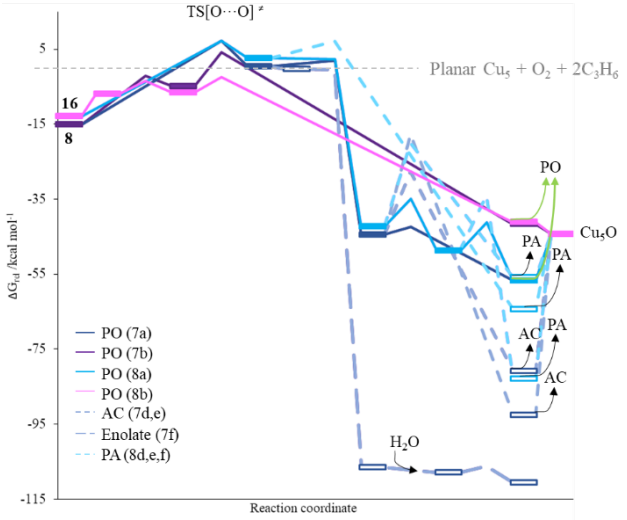


**Figure 9.** Free energy profiles for the transformation of OMC intermediates **8** and **16** into PO (full lines) or secondary products (dashed lines). The pathways are depicted in Figures 7 and 8. The origin of energies corresponds to separate planar $Cu_5$+$O_2$+ 2propene.

Regarding LH mechanisms from structure **53** (see Figure 10b), we found that adsorption of propene yielding structures **117** and **120** is strong, -21 kcal mol$^{-1}$, but the formation of the OMC intermediates **119** and **122** requires activation energies larger than 40 kcal mol$^{-1}$, making this process highly improbable. The reason for such large barriers is that, in structures **117** and **120,** propene is far from the tri-coordinated oxygen atom and the reaction requires the detachment of the Cu atom at which propene is bonded, thus destabilizing transition states **118** and **121**. In contrast, the reaction towards allyl is not so impeded sterically and the activation energy is affordable, 22.9 kcal mol$^{-1}$. But since the ER path to form PO from structure **53** requires 22.3 kcal mol$^{-1}$, it will remain slightly predominant. In addition, the production of PO through the more favourable pathways in the first part of the cycle ultimately yields structure **72**, as opposed to structure **53** (Figures 7, 8). This way, the possible decrease of selectivity associated to propene adsorption on structure **53** before reacting through the more favourable ER mechanism, is avoided or at least minimized.

## 4. CONCLUSIONS

The mechanism of propene epoxidation with either molecular $O_2$ or atomic O catalysed by planar and 3D $Cu_5$ clusters has been theoretically investigated in order to establish whether the cluster morphology and the nature of the oxygen species present has an influence on the selectivity of the reaction.

In the first part of the mechanism, the less nucleophilic character of $O_2$ adsorbed in a *bridge* mode on planar $Cu_5$ clusters leads to the preferential formation of OMC intermediates precursors of PO. In contrast, 3D $Cu_5$ clusters allow the adsorption of $O_2$ in a more activating *h-111* mode, i.e. as a superoxo species, whose basicity is high enough to favour the abstraction of a hydrogen atom from the methyl group thus leading to an allyl intermediate. Moreover, $O_2$ dissociation is easy on 3D $Cu_5$ clusters, and the resulting adsorbed O atoms preferentially react with the methyl hydrogens of co-adsorbed propene producing allyl species. In the second part of the mechanism, the OMC intermediates formed on planar $Cu_5$ clusters evolve to PO with activation energy barriers systematically lower than those required to form undesired acetone or propanal.

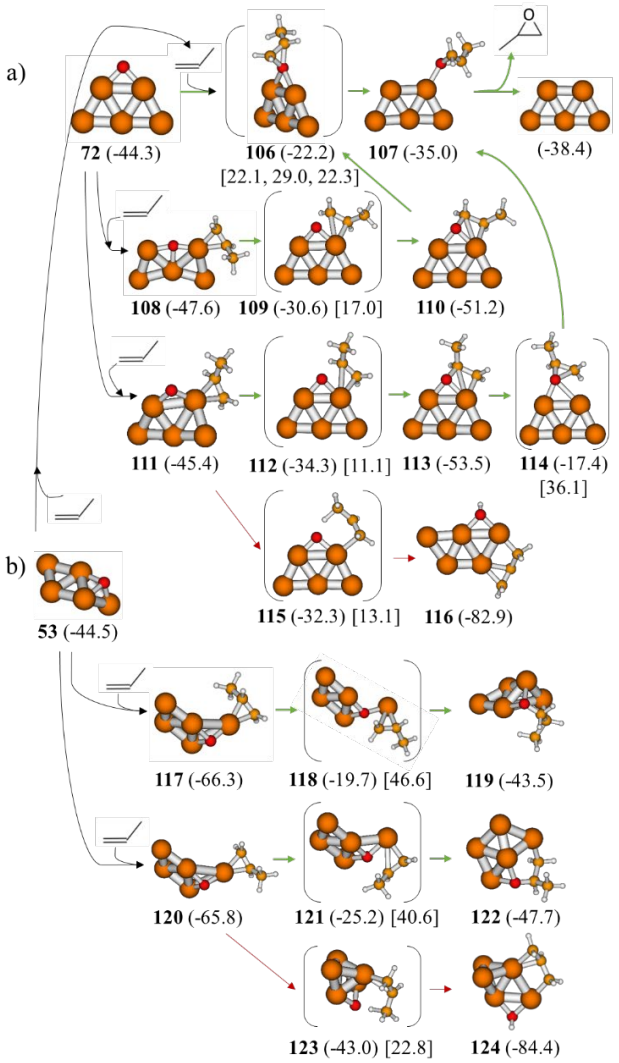


**Figure 10.** Optimized structures involved in the formation of OMC and allyl intermediates on $Cu_5O$ systems. Relative Gibbs free energies with respect to separate planar $Cu_5$+$O_2$+2$C_3H_6$ (in parenthesis) and activation Gibbs free energies for elementary steps (in square brackets) in kcal mol$^{-1}$. Cu, C, O and H atoms depicted in orange, amber, red and white, respectively.

After formation and desorption of the first PO molecule, the resulting $Cu_5O$ structure must react with a second propene molecule to close the catalytic cycle. In this case, the direct formation of a second PO molecule following an Eley-Rideal mechanism competes with allyl formation due to the planar geometry of the $Cu_5$ cluster, which stabilizes the $Cu^0$ metallic state. In spite of some minor deformations through the process, at the end of the reaction the cluster preserves its planar geometry, thus enabling a new catalytic cycle without loss of activity or selectivity. Note that since morphology and the resulting electronic structure of planar $Cu_5$ is a key factor for the selectivity of the reaction towards PO, experimental trials on the application of this catalyst should employ a support able to stabilize planar $Cu_5$ clusters without altering their electronic and hence their catalytic properties.[33] On the other hand, the fact that the planar isomer is 7.8 kcal mol$^{-1}$ more stable than the 3D isomer in gas phase[31] should facilitate the reaction to PO.

## AUTHOR INFORMATION


### Corresponding Author

Mercedes Boronat, boronat@itq.upv.es

**ORCID**

Estefanía Fernández: 0000-0002-9419-0786
Avelino Corma: 0000-0002-2232-3527
Mercedes Boronat: 0000-0002-6211-5888


**Notes**

The authors declare no competing financial interest.

**Supporting Information.** Bond distances and NBO charges of all structures, and correlation between activation energies and charges on O atoms.

## ACKNOWLEDGMENT


This work has been supported by the European Union through ERC-AdG-2014-671093 (SynCatMatch) and by Spanish Government through ''Severo Ochoa" (SEV-2016-0683, MINECO) and MAT2017-82288-C2-1-P (AEI/FEDER, UE) Projects. E.F.V. thanks Spanish MINECO for her fellowship SVP-2013-068146.


## REFERENCES


(1) Lambert, R. M.; Williams, F. J.; Cropley, R. L.; Palermo, A. Heterogeneous Alkene Epoxidation: Past, Present and Future. *J. Mol. Catal. A Chem.* **2005**, *228* (1–2), 27–33.

(2) Nijhuis, T. A.; Makkee, M.; Moulijn, J. A.; Weckhuysen, B. M. The Production of Propene Oxide: Catalytic Processes and Recent Developments. *Ind. Eng. Chem. Res.* **2006**, *45* (10), 3447–3459.

(3) Sheldon, R. A. E Factors, Green Chemistry and Catalysis: An Odyssey. *Chem. Commun.* **2008**, No. 29, 3352.

(4) Khatib, S. J.; Oyama, S. T. Direct Oxidation of Propylene to Propylene Oxide with Molecular Oxygen: A Review. *Catal. Rev.* **2015**, *57* (3), 306–344.

(5) Clerici, M.; Bellusi, G.; Romano, U. Synthesis of Propylene Oxide from Propylene and Hydrogen Peroxide Catalyzed by Titanium Silicalite. *J. Catal.* **1991**, *129* (1), 159–167.

(6) Huang, J.; Haruta, M. Gas-Phase Propene Epoxidation over Coinage Metal Catalysts. *Res. Chem. Intermed.* **2012**, *38* (1), 1–24.

(7) Lee, W.-S.; Lai, L.-C.; Cem Akatay, M.; Stach, E. A.; Ribeiro, F. H.; Delgass, W. N. Probing the Gold Active Sites in Au/TS-1 for Gas-Phase Epoxidation of Propylene in the Presence of Hydrogen and Oxygen. *J. Catal.* **2012**, *296*, 31–42.

(8) Chen, J.; Halin, S. J. A.; Pidko, E. A.; Verhoeven, M. W. G. M. T.; Ferrandez, D. M. P.; Hensen, E. J. M.; Schouten, J. C.; Nijhuis, T. A. Enhancement of Catalyst Performance in the Direct Propene Epoxidation: A Study into Gold-Titanium Synergy. *ChemCatChem* **2013**, *5* (2), 467–478.

(9) LLORCA, J.; DOMINGUEZ, M.; LEDESMA, C.; CHIMENTAO, R.; MEDINA, F.; SUEIRAS, J.; ANGURELL, I.; SECO, M.; ROSSELL, O. Propene Epoxidation over TiO2-Supported Au–Cu Alloy Catalysts Prepared from Thiol-Capped Nanoparticles. *J. Catal.* **2008**, *258* (1), 187–198.

(10) Li, Z.; Gao, L.; Zhu, X.; Ma, W.; Feng, X.; Zhong, Q. Synergistic Enhancement over Au-Pd/TS-1 Bimetallic Catalysts for Propylene Epoxidation with H 2 and O 2. *ChemCatChem* **2019**, *11* (20), 5116–5123.

(11) Jenzer, G.; Mallat, T.; Maciejewski, M.; Eigenmann, F.; Baiker, A. Continuous Epoxidation of Propylene with Oxygen and Hydrogen on a Pd–Pt/TS-1 Catalyst. *Appl. Catal. A Gen.* **2001**, *208* (1–2), 125–133.

(12) Voge, H. H.; Adams, C. R. Catalytic Oxidation of Olefins; 1967; pp 151–221.

(13) Kilty, P. A.; Sachtler, W. M. H. THE MECHANISM OF THE SELECTIVE OXIDATION OF ETHYLENE TO ETHYLENE OXIDE. *Catal. Rev.* **1974**, *10* (1), 1–16.

(14) Serafin, J.; Liu, A.; Seyedmonir, S. Surface Science and the Silver-Catalyzed Epoxidation of Ethylene: An Industrial Perspective. *J. Mol. Catal. A Chem.* **1998**, *131*, 157–168.

(15) LU, J.; BRAVOSUAREZ, J.; TAKAHASHI, A.; HARUTA, M.; OYAMA, S. In Situ UV–Vis Studies of the Effect of Particle Size on the Epoxidation of Ethylene and Propylene on Supported Silver Catalysts with Molecular Oxygen. *J. Catal.* **2005**, *232* (1), 85–95.

(16) Lei, Y.; Mehmood, F.; Lee, S.; Greeley, J.; Lee, B.; Seifert, S.; Winans, R. E.; Elam, J. W.; Meyer, R. J.; Redfern, P. C.; Teschner, D.; Schlogl, R.; Pellin, M. J.; Curtiss, L. A.; Vajda, S. Increased Silver Activity for Direct Propylene Epoxidation via Subnanometer Size Effects. *Science (80-. ).* **2010**, *328* (5975), 224–228.

(17) Molina, L. M.; Lee, S.; Sell, K.; Barcaro, G.; Fortunelli, A.; Lee, B.; Seifert, S.; Winans, R. E.; Elam, J. W.; Pellin, M. J. Size-Dependent Selectivity and Activity of Silver Nanoclusters in the Partial Oxidation of Propylene to Propylene Oxide and Acrolein: A Joint Experimental and Theoretical Study. *Catal. Today* **2011**, *160* (1), 116–130.

(18) Pulido, A.; Concepción, P.; Boronat, M.; Corma, A. Aerobic Epoxidation of Propene over Silver (111) and (100) Facet Catalysts. *J. Catal.* **2012**, *292*, 138–147.

(19) Boronat, M.; Pulido, A.; Concepción, P.; Corma, A. Propene Epoxidation with O 2 or H 2 –O 2 Mixtures over Silver Catalysts: Theoretical Insights into the Role of the Particle Size. *Phys. Chem. Chem. Phys.* **2014**, *16* (48), 26600–26612.

(20) Torres, D.; Lopez, N.; Illas, F.; Lambert, R. M. Low-Basicity Oxygen Atoms: A Key in the Search for Propylene Epoxidation Catalysts. *Angew. Chemie Int. Ed.* **2007**, *46* (12), 2055–2058.

(21) Roldan, A.; Torres, D.; Ricart, J. M.; Illas, F. On the Effectiveness of Partial Oxidation of Propylene by Gold: A Density Functional Theory Study. *J. Mol. Catal. A Chem.* **2009**, *306* (1–2), 6–10.

(22) VAUGHAN, O.; KYRIAKOU, G.; MACLEOD, N.; TIKHOV, M.; LAMBERT, R. Copper as a Selective Catalyst for the Epoxidation of Propene. *J. Catal.* **2005**, *236* (2), 401–404.

(23) Greiner, M. T.; Jones, T. E.; Johnson, B. E.; Rocha, T. C. R.; Wang, Z. J.; Armbrüster, M.; Willinger, M.; Knop-Gericke, A.; Schlögl, R. The Oxidation of Copper Catalysts during Ethylene Epoxidation. *Phys. Chem. Chem. Phys.* **2015**, *17* (38), 25073–25089.

(24) Marimuthu, A.; Zhang, J.; Linic, S. Tuning Selectivity in Propylene Epoxidation by Plasmon Mediated Photo-Switching of Cu Oxidation State. *Science (80-. ).* **2013**, *339* (6127), 1590–1593.

(25) Su, W.; Wang, S.; Ying, P.; Feng, Z.; Li, C. A Molecular Insight into Propylene Epoxidation on Cu/SiO2 Catalysts Using O2 as Oxidant. *J. Catal.* **2009**, *268* (1), 165–174.

(26) Hua, Q.; Cao, T.; Gu, X.-K.; Lu, J.; Jiang, Z.; Pan, X.;

Luo, L.; Li, W.-X.; Huang, W. Crystal-Plane-Controlled Selectivity of Cu 2 O Catalysts in Propylene Oxidation with Molecular Oxygen. *Angew. Chemie Int. Ed.* **2014**, *53* (19), 4856–4861.

(27) Guo, L.-L.; Yu, J.; Shu, M.; Shen, L.; Si, R. Silicon Nitride as a New Support for Copper Catalyst to Produce Acrolein via Selective Oxidation of Propene with Very Low CO2 Release. *J. Catal.* **2019**, *380*, 352–365.

(28) Song, Y.-Y.; Wang, G.-C. A DFT Study and Microkinetic Simulation of Propylene Partial Oxidation on CuO (111) and CuO (100) Surfaces. *J. Phys. Chem. C* **2016**, *120* (48), 27430–27442.

(29) Song, Y.-Y.; Dong, B.; Wang, S.-W.; Wang, Z.-R.; Zhang, M.; Tian, P.; Wang, G.-C.; Zhao, Z. Selective Oxidation of Propylene on Cu 2 O(111) and Cu 2 O(110) Surfaces: A Systematically DFT Study. *ACS Omega* **2020**, *5* (12), 6260–6269.

(30) Xiao, T.-T.; Li, R.-S.; Wang, G.-C. A DFT Study and Microkinetic Simulation in Propylene Oxidation on the "29" Cu x O/Cu(111) Surface. *J. Phys. Chem. C* **2020**, *124* (12), 6611–6623.

(31) Fernández, E.; Boronat, M.; Corma, A. Trends in the Reactivity of Molecular O 2 with Copper Clusters: Influence of Size and Shape. *J. Phys. Chem. C* **2015**, *119* (34), 19832–19846.

(32) Concepción, P.; Boronat, M.; García-García, S.; Fernández, E.; Corma, A. Enhanced Stability of Cu Clusters of Low Atomicity against Oxidation. Effect on the Catalytic Redox Process. *ACS Catal.* **2017**, *7* (5), 3560–3568.

(33) Fernández, E.; Boronat, M. Sub Nanometer Clusters in Catalysis. *J. Phys. Condens. Matter* **2019**, *31* (1), 013002.

(34) Frisch, M. J.; Trucks, G. W.; Schlegel, H. B.; Scuseria, G. E.; Robb, M. A.; Cheeseman, J. R.; Scalmani, G.; Barone, V.; Mennucci, B.; Petersson, G. A.; Nakatsuji, H.; Caricato, M.; Li, X.; Hratchian, H. P.; Izmaylov, A. F.; Bloino, J.; Zheng, G.; Sonnenberg, J. L.; Had, M.; Fox, D. J. Gaussian 09. Gaussian, Inc.: Wallingford CT 2009.

(35) Becke, A. D. Density-functional Thermochemistry. III. The Role of Exact Exchange. *J. Chem. Phys.* **1993**, *98* (7), 5648–5652.

(36) Weigend, F.; Ahlrichs, R. Balanced Basis Sets of Split Valence, Triple Zeta Valence and Quadruple Zeta Valence Quality for H to Rn: Design and Assessment of Accuracy. *Phys. Chem. Chem. Phys.* **2005**, *7* (18), 3297.

(37) Weigend, F. Accurate Coulomb-Fitting Basis Sets for H to Rn. *Phys. Chem. Chem. Phys.* **2006**, *8* (9), 1057.

(38) Binkley, J. S.; Pople, J. A.; Hehre, W. J. Self-Consistent Molecular Orbital Methods. 21. Small Split-Valence Basis Sets for First-Row Elements. *J. Am. Chem. Soc.* **1980**, *102*, 939–947.

(39) Reed, A. E.; Weinstock, R. B.; Weinhold, F. Natural Population Analysis. *J. Chem. Phys.* **1985**, *83* (2), 735–746.

(40) Schaftenaar, G.; Noordik, J. H. Molden: A Pre- and Post-Processing Program for Molecular and Electronic Structures*. *J. Comput. Aided. Mol. Des.* **2000**, *14*, 123–134.

(41) Http://Www.Jmol.Org/.

(42) Adrienko, G. A. Chemcraft. http://Www.Chemcraftprog.Com.

# The crucial role of cluster morphology on the epoxidation of propene catalyzed by $Cu_5$: a DFT study

Estefanía Fernández, Mercedes Boronat,* and Avelino Corma

Instituto de Tecnología Química, Universitat Politècnica de València - Consejo Superior de Investigaciones Cientificas, Av. de los Naranjos, s/n, 46022 Valencia, Spain

Insert Table of Contents artwork here